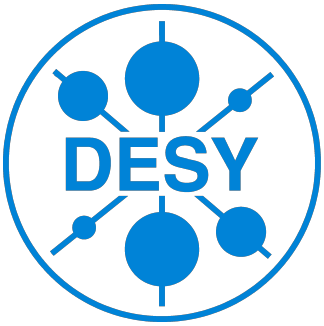

Positivity Violation of Double Parton Distributions under Scale Evolution

Paolo Pichini, University of Manchester, UK

Supervisor: Markus Diehl

September 6, 2017

Abstract

In this work we study double parton distributions (DPDs) in hadron-hadron collisions, focussing on the properties that arise due to colour. In particular, we check whether the DPDs stay positive semidefinite under the scale evolution given by the DGLAP equations. A similar analysis on single parton distributions (J. C. Collins *et al*, C. Bourrely *et al*) and colour-singlet DPDs (M. Diehl and T. Kasemets) found that positivity is preserved, as naively expected given the probabilistic interpretation of such functions. Nevertheless we find that including the full colour structure, positivity does not have to be preserved for a general DPD, and we provide examples where it is violated.

Contents

1 Introduction

1.1 Parton distribution functions

In current particle physics experiments, hadron-hadron collisions are often investigated. In such cases, the interactions will occur between the fundamental constituents of the hadrons: quarks and gluons, known as *partons*.
In computing cross-sections we are interested in the so-called *hard processes*, interactions between partons with high energy and transverse momentum, which will produce high energy final states (for instance leptons) that can be observed in the detectors. The most common scenario in a hadron-hadron collision is that of a single hard process, plus other low energy interactions, and we will initially focus on this.
An important result is the *factorisation theorem*, which roughly states that the probability of a certain final state is given by the product between the hard subprocess cross section and functions encoding the information about the initial distribution of partons inside the hadron. Such functions are known as *parton distribution functions (PDF)* or *parton densities*, and they give the probability of a certain parton having some fraction x of the hadron momentum at time of collision.
In QCD, the PDFs additionally depend on the scale of the hard process. Indeed, there are contributions which introduce collinear and UV divergences (see Fig.1) and the PDF must be renormalised to account for these. In particular, in Fig.1(left) collinear divergences from low p_T contributions (compared to the scale of the hard process) are absorbed into the PDF, whereas the high p_T contributions are included in the hard process. UV divergences from Fig.3(right) also have to be subtracted. This introduces a scale dependence which obeys the DGLAP evolution equations [1].

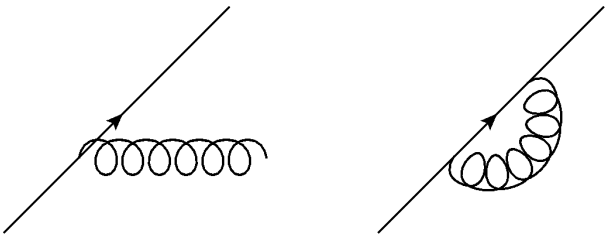

Figure 1: Example of diagrams contributing to the overall amplitude which play a role in the PDF renormalisation.

It is natural to wonder whether the scale dependence affects the positivity of the PDFs and hence their interpretation as probability densities. This topic has been widely studied and it was shown that positivity is preserved by the scale evolution (see for instance [2, 3]), assuming leading order splitting kernels (see later).

1.2 Double parton distributions

When two hadrons collide at very high energies, it is possible that two or more hard processes will occur between the partons. Such multiparton interactions have been studied since a long time ago [4, 5] and they have been experimentally observed at Tevatron and at the LHC (see for instance [6–10]).
Substantial work has been done to extend the PDF formalism to the case of two hard processes, known as *double parton scattering (DPS)*. In this case, the total cross-section will depend on the initial distribution of dipartonic states in each hadron. This can be encoded in *double parton distributions (DPDs)* which—extending factorisation to DPS—can be combined with the cross-sections for the two hard processes to obtain the total cross-section for the interaction.
Examples of early work on DPDs are [11–13]. In later years more systematic descriptions of multiparton interactions have been produced, including [14–17], and our understanding of DPDs has been consolidated.
Figure 2 illustrates how DPDs are implemented, assuming factorisation. The cut diagram is a standard notation in high energy physics: it separates the amplitude of a process from its conjugate amplitude and it is a way of computing the probability of said process summed over all possible final states. The green blobs hide the inner workings of the colliding hadrons and their contribution to the cross-section is given by the DPDs. The grey circles represent the hard scattering between the partons (in this case, a quark, an antiquark and two gluons) and are computed independently of the hadron's initial conditions.

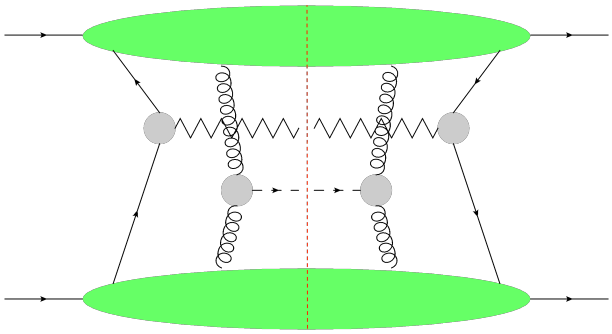

Figure 2: Example of double hard scattering in hadron-hadron collisions. The green blobs represent the hadrons and the grey circles are the vertices of the hard processes.

The scale evolution of DPDs can be expressed by the DGLAP equations as in the single parton case. The difference is that, since there are two hard processes, there will be two separate scales. In other words, for each of the two partons the contributions shown in Fig.1 must be absorbed in the DPD, and how many contributions will be absorbed depends on the scale of the single hard process of the parton considered.

As outlined in [13], DPDs depend not only on the fractional momenta of the two partons, but also on their relative transverse distance and on the colour and spin state of the diparton system. It was shown that, considering colour-singlet distributions (or ignoring the colour structure of DPDs), positivity is preserved under scale evolution just like in the case of PDFs [18]. The present work considered the full colour structure of unpolarised distributions, to see if the same result could be obtained in this case.

2 Theory

The aim of this section is to show that PDFs and DPDs can be expressed as density matrices in colour space, and discuss two different bases for such matrices. In one such basis the coefficients will correspond to probabilities (at least before renormalisation), and hence their behaviour under evolution will be investigated. The second basis will instead be useful in writing down the evolution equations. For simplicity we will assume that the colliding hadrons are protons, but the analysis applies to other cases too.

2.1 Parton distributions as density matrices

2.1.1 Single parton distributions

The local gauge symmetry of QCD is given by the group SU(3), associated to the colour charge. Each object within the theory—such as a quark state or a gluon field—will transform under a certain representation of SU(3). For instance, quark states can be written as a complex 3-vector transforming under the fundamental representation, with respect to which SU(3) is just the group of 3×3 unitary matrices.
Parton distribution functions give the probability of finding a parton state ψ within a proton. For any given parton, such a probability can be written as

$$P(\psi) = \sum_X \mathcal{A}(p \to \psi + X)\mathcal{A}^*(p \to \psi + X) \tag{1}$$

where $\mathcal{A}(p \to \psi + X)$ is the amplitude for a proton giving the single parton state ψ and a final state X of the other partons. The total probability is found summing over all possible X, and it is represented via the usual cut-diagram in Fig.3. Since the state ψ is a linear combination of color basis states $\{i\}$ and since the amplitude is linear with respect to the colour state, we can rewrite this as

$$P(\psi) = (\psi^i)^* \psi^{i'} f^{ii'} \tag{2}$$

where

$$f^{ii'} = \sum_X \mathcal{A}(p \to i + X)\mathcal{A}^*(p \to i' + X). \tag{3}$$

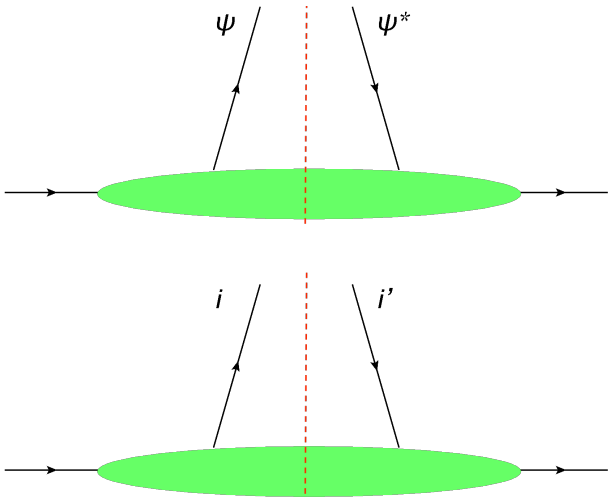

Figure 3: The top diagram represents the probability to find the state ψ inside the proton. The bottom diagram corresponds to $f^{ii'}$.

The tensor $f^{ii'}$ is by definition a density matrix. It has two colour indices, the non-primed one belonging to the amplitude and the primed one to the conjugate amplitude. Such indices must transform in the opposite way to the ones they are contracted with, since the probability must be gauge invariant. Hence, if the state ψ belongs to some representation R, $f^{ii'}$ must be a member of the product space $R \otimes \overline{R}$, since the two indices transform like ψ and ψ^* respectively.
In addition, it can be shown that since the hadron is a colour singlet and the probability is summed over all possible final states, $f^{ii'}$ must be a colour singlet. In the case of single parton scattering the only option is

$$f^{ii'} = \frac{f_1}{\dim(R)}\,\delta^{ii'} \tag{4}$$

where f_1 is in general a complex number. By taking the trace (i.e. summing over all colour base states) we can see that f_1 is the total probability of finding the parton considered in the hadron.

2.1.2 Double parton distributions

The same arguments outlined above apply in the case of DPS, although in this case the number of indices will double. We can denote with Ψ the diparton state we wish to compute the probability of. This will have two colour indices (in component notation, $\Psi^{\ell_1\ell_2}$), each being associated to a quark, an antiquark or a gluon and transforming accordingly.
Eq.1 is still valid, and exploiting the linearity of the amplitude we can rewrite it as:

$$P(\Psi) = (\Psi^{\ell_1\ell_2})^* \Psi^{\ell_1'\ell_2'} F^{\ell_1\ell_2\ell_1'\ell_2'}. \tag{5}$$

Here $F^{\ell_1\ell_2\ell'_1\ell'_2}$ belongs to a more complicated product space, formed by the representations associated to each index. Again, the non-primed indices belong to the amplitude and the primed ones to the conjugate amplitude. Our goal is to expand the density matrix in terms of a basis for the product space, using the fact that it must be a colour singlet. To show an example of how this can be done, we will consider a diparton system formed by two quarks. We can relabel the indices as $F^{iji'j'}$ to highlight that they are (anti)quark indices. Although the following arguments can be extended to any diparton system, a more detailed and general analysis is given in [13].
Each quark belongs to the fundamental representation of SU(3), which we will denote as '3' (from its dimensionality). To obey the right transformation laws, $F^{iji'j'}$ (shown by Fig.4) must have two quark-like indices and to anti-quark like indices [1]. In other words, it must belong to the space $3\otimes 3\otimes\bar{3}\otimes\bar{3}$, where '$\bar{3}$' denotes the conjugate representation.

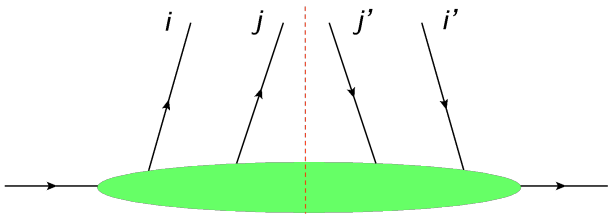

Figure 4: Diagrammatic representation of the matrix element $F^{iji'j'}$. It is evident that the indices i and j are quark indices whereas the others are anti-quark indices.

To find a convenient basis for such a space, we first consider the product spaces $3\otimes 3$ and $\bar{3}\otimes\bar{3}$ separately. Via a standard group-theoretical analysis, we can decompose such spaces into irreducible representations, finding that $3\otimes 3=\bar{3}\oplus 6$ and by conjugation $\bar{3}\otimes\bar{3}=3\oplus\bar{6}$. Note that since $3\otimes 3$ is the space of double quark states Ψ, we can conclude that Ψ must be an anti-triplet or a sextet (or linear combinations) under SU(3).
Therefore, we can write $3\otimes 3\otimes\bar{3}\otimes\bar{3}=(\bar{3}\oplus 6)\otimes(3\oplus\bar{6})=(\bar{3}\otimes 3)\oplus(\bar{3}\otimes\bar{6})\oplus(6\otimes 3)\oplus(6\otimes\bar{6})$. It can be then be shown that only two (basis) singlets can be obtained from this decomposition, one from $\bar{3}\otimes 3$ and another from $6\otimes\bar{6}$. A general colour singlet in the space can be expressed in terms of these, and hence we can rewrite the density matrix as:

$$F^{iji'j'}=\frac{1}{6}F_{\bar{3}}(\delta^{ii'}\delta^{jj'}-\delta^{ij'}\delta^{ji'})+\frac{1}{12}F_6(\delta^{ii'}\delta^{jj'}+\delta^{ij'}\delta^{ji'}) \tag{6}$$

where the matrix elements for the basis singlets (known as *projection operators*) and the normalisations have been taken from [13, Eq.7-12]. It can also be shown (see again [13]) that the coefficients F_R correspond to the probability of finding two quarks in the representation R ($\bar{3}$ or 6), in a similar way to what we outlined for single parton densities. This interpretation is not limited to the double quark densities but generalises to any

[1] Recall that an object in the fundamental representation, when complex-conjugated, will give an object in the conjugate representation (see Eq.5).

DPD. Hence, these coefficients are naively expected to be positive definite functions of the fractional momenta x_1 and x_2 of the two partons, and to preserve their positivity under evolution.
When decomposing the space $3\otimes 3\otimes\bar{3}\otimes\bar{3}$, we could have taken a different approach. We could first write $3\otimes\bar{3} = 1\oplus 8$ and then $3\otimes 3\otimes\bar{3}\otimes\bar{3} = (3\otimes\bar{3})\otimes(3\otimes\bar{3}) = (1\oplus 8)\otimes(1\oplus 8) = (1\otimes 1)\oplus(8\otimes 1)\oplus(1\otimes 8)\oplus(8\otimes 8)$. In this case it is straightforward to see that $1\otimes 1$ corresponds to a unique singlet state and that $1\otimes 8 = 8\otimes 1 = 8$ will only contain octet states. It can be shown that another singlet can come from the $8\otimes 8$ space. Hence we can express $F^{iji'j'}$ in terms of this alternative basis:

$$F^{iji'j'} = \frac{1}{9}({}^1F\delta^{ii'}\delta^{jj'} + \frac{3}{\sqrt{2}}{}^8F t_a^{ii'}t_a^{jj'}) \tag{7}$$

where the new projection operators and their normalisation were taken from [19]. By contracting this expression with the previous projection operators, it is possible obtain a change of basis matrix $\mathcal{C}$ that relates the coefficients ${}^RF$ and F_R. Denoting $\vec{F}$ a column vector with a set of coefficients, we can write:

$$\vec{F}_R = \mathcal{C}\ {}^R\vec{F}. \tag{8}$$

This will turn out be be quite useful, as it will allow the evolution of $\vec{F}_R$ to be expressed via the (simpler) evolution of ${}^R\vec{F}$. More details will be given in the next subsection.

2.2 Scale evolution

As mentioned in the introduction, parton distributions must be renormalised to avoid divergences such as those in Fig.1, represented via the usual cut-diagram in Fig.5. This implies reabsorbing into them all diagram contributions with transverse momentum significantly lower than the scale of the hard scattering, plus diverging virtual graphs, rather than computing them as part of the hard scattering amplitude. In Fig.5 this is represented as the extension of the green oval to include such diverging processes (see green dotted line).
Mathematically, the evolution is given by the DGLAP equations. For single parton densities we write

$$\frac{\partial f(x,\tau)}{\partial\tau} = \int_x^1 \frac{dy}{y} P(\frac{x}{y}) f(y,\tau) \tag{9}$$

where $f(x,\tau)$ corresponds to f_1 in Eq.4. The evolution parameter τ is given by:

$$\tau = \int_{C^2}^{\mu^2} \frac{d\mu'^2}{\mu'^2}\frac{\alpha_S(\mu')}{2\pi} \tag{10}$$

where μ is the scale of the hard process and C is an arbitrary constant. The function $P(x/y)$ is known as *splitting kernel* and it can be interpreted as proportional to the probability that a parton with fractional momentum y loses energy (e.g. emits a gluon) and is left with fractional momentum x. Therefore, Eq.9 roughly states that the change

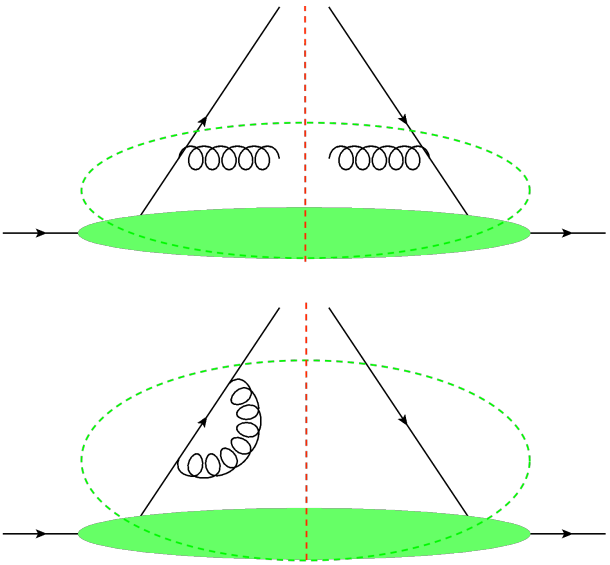

Figure 5: Some leading order diagrams contributing to the overall cross section which are accounted for in the parton distribution.

in the density of partons with fractional momentum x at a certain scale μ depends on how likely it is for partons with higher momentum to radiate away some of their energy at that scale (i.e. within the diagrams absorbed into the PDF).
In Fig.5, the added contribution to the quark density comes from a higher energy quark radiating a gluon. However, another contribution to the quark density could be given by a gluon turning into a quark-antiquark pair. It is clear that Eq.9 must be rewritten to include such cases. First, we can define a shorthand notation for the convolution in Eq.9:

$$P_{ab} \otimes f_b(x,\tau) \equiv \int_x^1 \frac{dy}{y} P_{ab}(\frac{x}{y}) f_b(y,\tau). \tag{11}$$

The indices have been added to highlight that we are considering a density for partons of type b (e.g. f_q for quarks) and a splitting function giving the probability that partons of type b evolve into partons of type a. Using this notation, we can generalise Eq.9 as follows:

$$\frac{\partial f_a(x,\tau)}{\partial \tau} = \sum_b P_{ab} \otimes f_b(x,\tau). \tag{12}$$

We now wish to extend this analysis to DPDs. A DPD is a function of the form $F_{a_1 a_2}(x_1, x_2, \tau_1, \tau_2)$, describing two partons of type a_1 and a_2 having momenta x_1 and x_2 at scales τ_1 and τ_2. It can be shown that such functions obey an evolution equation of the same form as Eq.9 with respect to each of the scales τ_i [14, sect 5.3.2]. However, there are additional complications. Let's take for instance the formulation of the density

matrix given by Eq.6. As mentioned, the (non-renormalised) coefficients are probabilities to find two partons in the representation R. If one of the partons radiates a gluon as in Fig.5, the representation of the diparton state could change in order to conserve colour. This implies that the scale evolution of a single F_R can also depend on the other coefficients. Combinining this to the possibility of different parton types, as given in Eq.12, we obtain fairly complicated evolution equations.
Let's consider Eq.7 instead. In this case, we have coupled each parton with its conjugate partner, and found a basis associated to the representations for this coupling. Any radiation process like the one in Fig.5 will be (mathematically) internal to the parton-antiparton pair, and hence colour conservation forbids it to change the pair's representation. In other words, the evolution of ${}^{R}F$ can only depend on coefficients associated to the representation R. Hence, we can write the equivalent of Eq.12 for DPDs in this basis:

$$\frac{\partial {}^{R}F_{a_1a_2}}{\partial \tau_1} = \sum_b {}^{R}P_{a_1b} \otimes_1 {}^{R}F_{ba_2}, \tag{13}$$

$$\frac{\partial {}^{R}F_{a_1a_2}}{\partial \tau_2} = \sum_b {}^{R}P_{a_2b} \otimes_2 {}^{R}F_{a_1b}. \tag{14}$$

The subscripts on the convolution symbols indicate which variable among x_1 and x_2 should be considered for the convolution, which is still of the form given in Eq.11. In the rest of this work we will focus on Eq.13, since every argument also applies to the second case. To this purpose, we will use $\tau \equiv \tau_1$ and $x \equiv x_1$.
The single parton kernels of Eq.12 correspond to ${}^{1}P_{ab}$, since in that case the only possible parton-antiparton representation is a singlet. In addition, it can be shown that:

$${}^{R}P_{ab} = C_{ab}(R) {}^{1}P_{ab}^{real} + {}^{1}P_{ab}^{virt}, \tag{15}$$

where ${}^{1}P_{ab}^{real}$ and ${}^{1}P_{ab}^{virt}$ are the contributions to ${}^{1}P_{ab}$ from real and virtual diagrams respectively (see Fig.5). The coefficients $C_{ab}(R)$ are numbers and can be found in [17, sect 7.3.5] for a range of cases. Trivially, $C_{ab}(1) = 1$.
The virtual contributions only occur when initial and final partons are the same, and they leave the fractional momentum of the parton unaffected. In other words, we can write:

$${}^{1}P_{ab}^{virt}(z) = P_\delta \, \delta_{ab} \, \delta(1-z) \tag{16}$$

where $P_\delta \in \mathbb{R}$. By performing the convolution as given in Eq.11, we find that:

$$\sum_b {}^{1}P_{a_1b}^{virt} \otimes {}^{R}F_{ba_2} = P_\delta \, {}^{R}F_{a_1a_2}. \tag{17}$$

Therefore we can rewrite Eq.13 as:

$$\frac{\partial {}^{R}F_{a_1a_2}}{\partial \tau} = (\sum_b C_{a_1b}(R) {}^{1}P_{a_1b}^{real} \otimes {}^{R}F_{ba_2}) + P_\delta \, {}^{R}F_{a_1a_2}. \tag{18}$$

In our analysis we will only consider distributions (or linear combinations of them) for which the sum over parton types b does not apply, since their evolution does not depend on other distributions. In this case, we can drop the indices and rewrite the above in a simpler form:

$$\frac{\partial^R F}{\partial \tau} = (C(R)^1 P_{real} \otimes {}^R F) + P_\delta \, {}^R F, \tag{19}$$

or, by defining $\mathcal{D} = \text{diag}(C(R_1), ..., C(R_n))$, we can express it in matrix form:

$$\frac{\partial^R \vec{F}}{\partial \tau} = \mathcal{D} \, ({}^1 P_{real} \otimes {}^R \vec{F}) + P_\delta \, {}^R \vec{F}. \tag{20}$$

Finally, we can combine Eq.8 and Eq.20 and obtain the evolution equations for the coefficients F_R:

$$\frac{\partial \vec{F}_R}{\partial \tau} = \mathcal{C} \, \mathcal{D} \, \mathcal{C}^{-1} \, ({}^1 P_{real} \otimes \vec{F}_R) + P_\delta \, \vec{F}_R. \tag{21}$$

We have now everything we need to investigate the positivity of the coefficients F_R. If we suppose that they are positive semidefinite functions of x_1 and x_2 at some $\tau = \tau_0$, we will deduce whether the scale evolution in Eq.21 must always preserve positivity or not. Note that we only consider an increase in τ, since going to too low scales would imply that the leading-order approximation to the splitting kernels is no longer accurate, hence there is no reason to expect conservation of positivity.

3 Results

Positivity is violated if it is possible that—if $F_R(x_1, x_2, \tau_0) = 0$ for some (x_1, x_2) and R—the τ-derivative of such a function at the same point is negative. Hence, we can see that the P_δ term in Eq.21 can be ignored, since if any of the F_R is zero, its contribution to the derivative will also be zero.
In our work we considered two cases: the flavour non-singlet distribution for two quarks and the double gluon distribution in a theory with no quarks. The details of each will be explored below. In both cases, it was found that the matrix $\mathcal{C} \, \mathcal{D} \, \mathcal{C}^{-1}$ contained only positive entries, hence the only possible source of positivity violation was the sign of ${}^1 P_{real} \otimes F_R$. We will show that ${}^1 P_{real} \otimes F_R$ can be negative for a general positive semidefinite F_R, and we will provide examples of initial conditions which lead to violation of positivity. In addition, we will show how these results can be extended to the full analysis of quark and gluons in QCD, by a suitable choice of initial conditions.

3.1 Double quark flavour non-singlet distribution

The flavour non-singlet distribution for two quarks can be defined as:

$$F_{vq} \equiv F_{uq} - F_{dq}, \tag{22}$$

where the second quark q could be any of the light quarks. At leading order, the following relations are valid for the splitting kernels:

$$\begin{cases} P_{uu} = P_{dd}\,, \\ P_{ug} = P_{dg}\,, \\ P_{ud} = P_{us} = P_{ds} = P_{q\bar{q}} = 0\,. \end{cases} \tag{23}$$

Hence, we can deduce the following:

$$\frac{\partial {}^{R}F_{vq}}{\partial \tau} = {}^{R}P_{uu} \otimes {}^{R}F_{vq}. \tag{24}$$

Hence, the evolution equations will be of the form given in Eq.21, since there is no contribution from other densities. For simplicity, we will use $F \equiv F_{vq}$ and $P \equiv P_{uu}$. The change of basis matrix $\mathcal{C}$ was calculated assuming the normalisations of Eq.6 and Eq.7:

$$\mathcal{C} = \frac{1}{3}\begin{pmatrix} 1 & -\sqrt{2} \\ 2 & \sqrt{2} \end{pmatrix}. \tag{25}$$

From [17, sect 7.3.5] we also found $\mathcal{D} = \mathrm{diag}(1, {}^{-1}\!/_{8})$. Together this yielded:

$$\mathcal{C}\,\mathcal{D}\,\mathcal{C}^{-1} = \frac{1}{8}\begin{pmatrix} 2 & 3 \\ 6 & 5 \end{pmatrix}. \tag{26}$$

As anticipated, all entries of the matrix are positive and hence positivity violation cannot arise due to this alone. Then, we computed ${}^{1}P_{real} \otimes F$ for two test functions:

$$F(x) = \frac{v - x}{x} \equiv f(x), \tag{27}$$

$$F(x) = \frac{v - x}{x}\,\cos^2 \pi x \equiv g(x). \tag{28}$$

As before, the variable x corresponds to x_1 in our analysis. Both functions are positive semidefinite and they satisfy the expected properties of a parton distribution: they diverge for $x = 0$ and they are zero for $x = v$, where $v = 1 - x_2$ is the maximum momentum available for the first parton. In addition $g(0.5) = 0$, which will be useful to test positivity. The convolution ${}^{1}P_{real} \otimes F(x, \tau)$ is given in [18, Appendix B]:

$$\lim_{\epsilon \to 0} \left(\int_{x+\epsilon}^{v} du \left[\frac{P_s(x/u)}{u - x} + \frac{P_r(x/u)}{u} \right] F(u, \tau) + \int_{0}^{x-\epsilon} du\, \frac{P_s(1)}{u - x}\, F(x, \tau) \right) \tag{29}$$

In this case $P_s(z) = C_F(1 + z^2)$ and $P_r(z) = 0$ [18, Appendix A]. Fig.6 shows the results for the two test functions of Eq.27 and Eq.28, using $v = 0.7$.

It is evident that ${}^{1}P_{real} \otimes F(x, \tau)$ can indeed be negative. Let's now check if this can affect the positivity of the F_R coefficients. In the double quark case we have $\vec{F}_R = (F_{\bar{3}}, F_6)^T$, as shown in Eq.6. We can take $F_{\bar{3}}(x) = g(x)$ and $F_6(x) = f(x)$ at $\tau = \tau_0$. Hence, at $x = 0.5$, $F_{\bar{3}}(x)$ is initially zero. We have ${}^{1}P_{real} \otimes f(0.5) \simeq -2.39443$ and ${}^{1}P_{real} \otimes g(0.5) \simeq 0.0486625$. We can compute the τ-derivative via Eq.21 using the matrix in Eq.26, and we find:

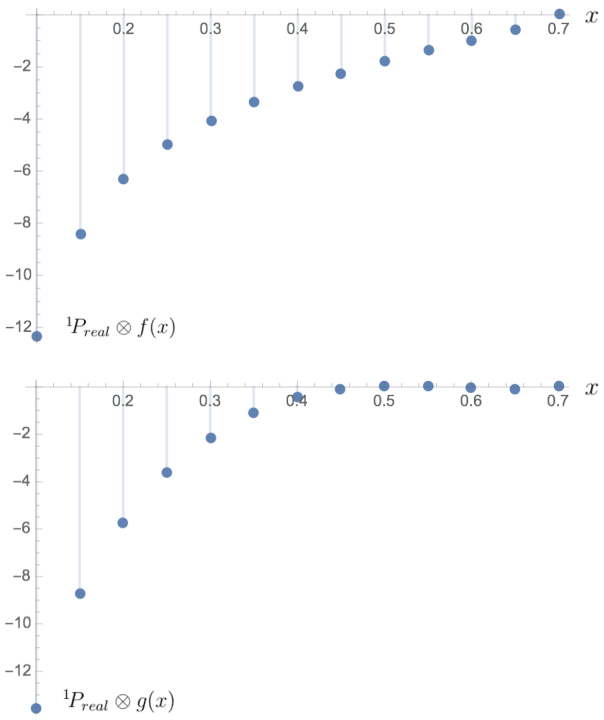

Figure 6: Plot of $^1P_{real} \otimes F(x)$ for the test functions $f(x)$ (top) and $g(x)$ (bottom), obtained using Wolfram Mathematica, in the case of double quark flavour non-singlet densities. To save calculations, only a few values have been computed.

$$\frac{\partial F_{\bar{3}}}{\partial \tau}(0.5, \tau_0) \simeq -0.885747\,. \tag{30}$$

This result was computed numerically using Mathematica with $\epsilon = 10^{-7}$. The same computation was performed for smaller ϵ, up to 10^{-11}, and the result did not change to the precision quoted. Hence, we can conclude that there are cases where initially positive semidefinite functions will become negative under scale evolution.

3.2 Double gluon distribution

The second case considered was that of a double gluon distribution in a quark-free theory. Since there are no other partons except for gluons, Eq.13 reduces to

$$\frac{\partial {}^R F_{gg}}{\partial \tau} = {}^R P_{gg} \otimes {}^R F_{gg}. \tag{31}$$

The gg subscripts can be dropped since there is no ambiguity. Gluons belong to the adjoint representation of SU(3), denoted '8'. Since $8 = \bar{8}$, the space for the density matrix (see Eq.5) will be $8 \otimes 8 \otimes 8 \otimes 8$. We have $8 \otimes 8 = 1 \oplus 8_s \oplus 8_a \oplus 10 \oplus \overline{10} \oplus 27$ yielding the allowed values of R. Since in both bases discussed earlier the decomposition

is of type $(8 \otimes 8) \otimes (8 \otimes 8)$, the same values will apply to both ${}^{R}F$ anf F_R. This is also true of the projection operators: the two bases are mathematically equivalent, and hence the operators will be the same up to normalisation—with the indices rearranged so that they belong to the right gluon.
It can be shown (see [19], Appendix A) that ${}^{10}F = {}^{\overline{10}}F$ and $F_{10} = F_{\overline{10}}$, thus reducing by one the number of degrees of freedom for the density matrix. Defining $F_D \equiv F_{10} + F_{\overline{10}}$, ${}^{D}F \equiv ({}^{10}F + {}^{\overline{10}}F)/\sqrt{2}$, $S \equiv 8_s$ and $A \equiv 8_a$, we can write ${}^{R}\vec{F} = ({}^{1}F, {}^{S}F, {}^{A}F, {}^{D}F, {}^{27}F)^T$ and $\vec{F}_R = (F_1, F_S, F_A, F_D, F_{27})^T$. The normalisation we used for F_R is from [13, Eq.7], whereas the one for ${}^{R}F$ is from [19, Eq.23]. In the former, the projection operator for F_D is the sum of the ones for F_{10} and $F_{\overline{10}}$, and the normalisation in Eq.7 will read $F_D/20$. In the latter, ${}^{D}F$ is denoted ${}^{(10+\overline{10})}F$.
Under such conditions, the change of basis matrix was computed:

$$\mathcal{C} \;=\; \frac{1}{64}\begin{pmatrix} 1 & 2\sqrt{2} & -2\sqrt{2} & 2\sqrt{5} & 3\sqrt{3} \\ 8 & -\frac{24\sqrt{2}}{5} & -8\sqrt{2} & -\frac{32}{\sqrt{5}} & \frac{24\sqrt{3}}{5} \\ 8 & 8\sqrt{2} & -8\sqrt{2} & 0 & -8\sqrt{3} \\ 20 & -16\sqrt{2} & 0 & 8\sqrt{5} & -4\sqrt{3} \\ 27 & \frac{54\sqrt{2}}{5} & 18\sqrt{2} & -\frac{18}{\sqrt{5}} & \frac{21\sqrt{3}}{5} \end{pmatrix}. \tag{32}$$

This differs from the change of basis found in [19] since the normalisation of F_R there is different, namely that of [13, Eq.6b]. The $C(R)$ coefficients were obtained from [17, sect 7.3.5], yielding $\mathcal{D} = \mathrm{diag}(1, 1/2, 1/2, 0, -1/3)$. Therefore we found:

$$\mathcal{C}\,\mathcal{D}\,\mathcal{C}^{-1} \;=\; \begin{pmatrix} 0 & 0 & \frac{1}{8} & 0 & 0 \\ 0 & \frac{1}{4} & \frac{1}{4} & \frac{1}{5} & 0 \\ 1 & \frac{1}{4} & \frac{1}{4} & 0 & \frac{1}{9} \\ 0 & \frac{1}{2} & 0 & \frac{1}{2} & \frac{2}{9} \\ 0 & 0 & \frac{3}{8} & \frac{3}{10} & \frac{2}{3} \end{pmatrix}. \tag{33}$$

As before, the matrix $\mathcal{C}\,\mathcal{D}\,\mathcal{C}^{-1}$ cannot be the only source of positivity violation since all entries are positive. Therefore, we calculated ${}^{1}P_{real} \otimes F(x)$ for the test functions in Eq.27 and Eq.28. The convolution was still in the form of Eq.29, but this time $P_s(z) = 6z$ and $P_r(z) = 6(1-z)(1+z^2)/z$ [18, Appendix A]. The results were similar to the double quark case and are shown in Fig.7.
We proceeded to find an example where positivity is violated. The evolution of F_R can be found by substituting Eq.33 into Eq.21. If at $\tau = \tau_0$ we take $F_R(x) = f(x)$ for $R \neq 1$, and $F_1(x) = g(x)$, we obtain

$$\frac{\partial F_1}{\partial \tau}(0.5, \tau_0) \simeq -0.666097\,, \tag{34}$$

but since $F_1(0.5, \tau_0) = g(0.5) = 0$, $F_1(0.5)$ will become negative. As before, we have shown that starting with a set of positive semidefinite functions that satisfy the typical properties of a parton distribution is not enough to guarantee that positivity will be

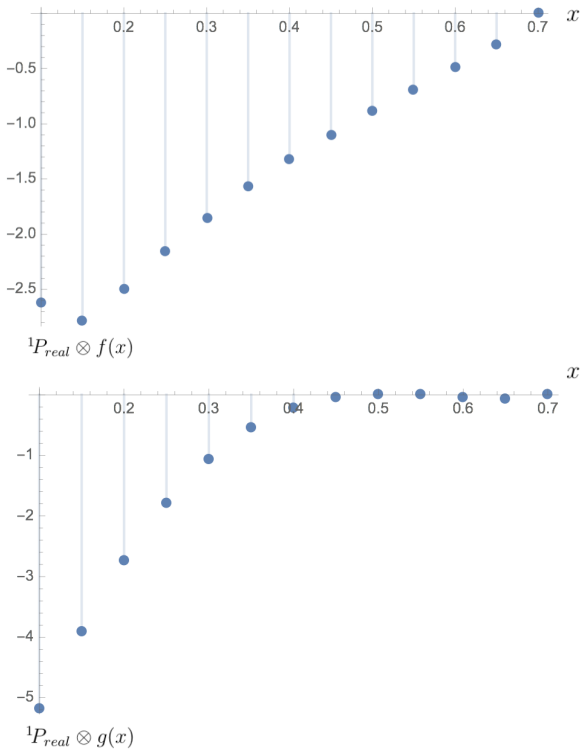

Figure 7: Plot of $^1P_{real} \otimes F(x)$ for the test functions $f(x)$ (top) and $g(x)$ (bottom), obtained using Wolfram Mathematica, in the case of double gluon densities. To save calculations, only a few values have been computed.

preserved at higher scales. The result of Eq.34 was also obtained numerically using Mathematica, for $\epsilon = 10^{-7}$. As before, repeating the calculation for values of ϵ down to 10^{-11} did not change the result to the precision quoted.

3.3 General DPDs in QCD

We will now show how the results given above can be extended to any double parton distribution in QCD. As before, the aim is to prove that starting with a set of positive semidefinite DPDs does not guarantee positivity will be preserved at higher scales.
The general evolution equation for the ^RF coefficients is given in Eq.13. We can define the column vector $^R\vec{F}_{tot} \equiv (^R\vec{F}_{qa_2}, ^R\vec{F}_{\bar{q}a_2}, ^R\vec{F}_{ga_2})^T$ containing all the relevant DPDs. Then Eq.13 can be written in matrix form:

$$\frac{\partial}{\partial \tau}(^R\vec{F}_{tot}) = \mathcal{P}\, ^R\vec{F}_{tot} \tag{35}$$

where $\mathcal{P}$ is a matrix containing the appropriate splitting kernels. Contrary to the previous cases $\mathcal{P}$ is not a diagonal matrix, as for instance $^RF_{ga_2}$ will contribute to the evolution

of ${}^{R}F_{qa_2}$ via ${}^{R}P_{qg}$ for any given R. Nonetheless, the full change of basis matrix $\mathcal{C}$ can be exploited to give

$$\frac{\partial}{\partial\tau}(\vec{F}_R^{\,tot}) = \mathcal{C}\,\mathcal{P}\,\mathcal{C}^{-1}\,\vec{F}_R^{\,tot}, \tag{36}$$

where $\vec{F}_R^{\,tot}$ is defined just like ${}^{R}\vec{F}_{tot}$ but with respect to the F_R coefficients. Now suppose we have $a_2 = g$. If we take as initial conditions $F^R_{a_1 g}(x,\tau_0) \propto \delta_{a_1 g}$ (here $F^R \equiv F_R$) we recover the same equations that we had for the gluon-gluon distributions in a quark-free theory (indeed here we are setting any (anti)quark-related distribution to zero, which is equivalent to saying that there are no (anti)quarks). Since $F(x) = 0$ is positive semidefinite, this implies that even Eq.36 does not preserve positivity for some set of initially positive semidefinite functions.
A similar argument applies to the case $a_2 = q$, since by setting $F^R_{a_1 q}(x,\tau_0) \propto \delta_{a_1 q}$ we obtain the same equations as in the case of double quark flavour non-singlet densities. Finally, the case $a_2 = \bar{q}$ is mathematically identical to $a_2 = q$, with the exception that quark and antiquark indices will be inverted. Therefore, the same arguments apply.

4 Conclusion

We have shown that, considering the full colour structure of unpolarised DPDs, there exist initially positive semidefinite distributions that will become negative under scale evolution. This was first proven for double quark flavour non-singlet distributions and gluon distributions in a quark-free theory, and then it was shown how the result can be generalised to any general DPD in QCD.
Such findings are fairly surprising, after previous results obtained for both single parton PDFs and DPDs [2, 3, 18]. A violation of positivity is however not sufficient to expect non-physical results in cross-section calculations. Indeed, in pp collisions the DPDs from both colliding protons will be present in the calculations. This implies summing quadratic terms such as $F_R^{(1)} F_R^{(2)}$ (the superscripts referring to the two protons) where even two negative parton distributions could give a positive contribution to the cross-section. On the other hand, the positivity of cross-sections is also not guaranteed, as for instance two parton distributions may be negative for non-matching values of x and hence yield a negative contribution at some x.
Besides, this work considered any set of positive semidefinite functions as possible initial conditions. Further work is needed to check in what cases a violation of positivity can arise and whether such cases can correspond to physical parton densities. To this purpose, the properties of ${}^{1}P_{real} \otimes F$ could be studied for a wider range of test functions F, to understand what conditions can lead to a negative result. A more complete analysis of the general case of DPDs in QCD, exploring the properties of Eq.36, may also provide interesting insight.
In summary, we found that the probabilistic interpretation of the F_R coefficients may not always be valid when considering the full colour structure of renormalised DPDs, but further work is required to test this hypothesis and understand its implications.

Acknowledgements

We thank Markus Diehl for the opportunity to work on this stimulating project and the constant and patient supervision he provided. We are also grateful to Maarten Buffing and Riccardo Nagar for the helpful discussions. We gratefully aknowledge the work of Olaf Behnke, the DESY Summer Programme 2017 organising team, the lecturers and the DESY summies for making such a pleasant and enriching experience possible.
The Feynman diagrams in this report were obtained using JaxoDraw [20].

References

[1] G. Altarelli and G. Parisi. Asymptotic freedom in parton language. *Nucl. Phys. B*, 126.

[2] J. C. Collins and J. Qiu. New derivation of the Altarelli-Parisi equations. *Phys. Rev. D*, 39:1398, 1989.

[3] C. Bourrely, J. Soffer, and O. V. Teryaev. The Q^2 evolution of Soffer inequality. *Phys. Rev. B*, 420:375, 1998.

[4] P.V. Landschoff, J.C. Polkinghorne, and D.M. Scott. Production of baryons with large transverse momentum. *Phys. Rev. D*, 12:3738, 1975.

[5] P.V. Landschoff and J.C. Polkinghorne. Calorimeter triggers for hard collisions. *Phys. Rev. D*, 18:3344, 1978.

[6] CDF collaboration, F. Abe, et al. Measurement of double parton scattering in $p\bar{p}$ collisions at $\sqrt{s} = 1.8$ TeV. *Phys. Rev. Lett.*, 79:584, 1997.

[7] D0 collaboration, V. M. Abazov, et al. Study of double parton interactions in diphoton + dijet events in $p\bar{p}$ collisions at $\sqrt{s} = 1.96$ TeV. *Phys. Rev. D*, 93:052008, 2016.

[8] LHCb collaboration, R. Aaij, et al. Production of associated y and open charm hadrons in pp collisions at $\sqrt{s} = 7$ and 8 TeV via double parton scattering. *J. High Energ. Phys.*, 2016:52, 2016.

[9] ATLAS collaboration, M. Aaboud, et al. Study of hard double-parton scattering in four-jet events in pp collisions at $\sqrt{s} = 7$ TeV with the atlas experiment. *J. High Energ. Phys.*, 2016:110, 2016.

[10] CMS collaboration, C. Chatrchyan, et al. Study of double parton scattering using W + 2-jet events in proton-proton collisions at $\sqrt{s} = 7$ TeV. *J. High Energ. Phys.*, 2014:32, 2014.

[11] N. Paver and D. Treleani. Multiquark scattering and large-p_T jet production in hadronic collisions. *D. Nuov Cim A*, 70:215, 1982.

[12] M. Mekhfi. Multiparton processes: an application to the double Drell-Yan mechanism. *Physical Review D*, 32(9):2371, 1985.

[13] M. Mekhfi. Correlations in color and spin multiparton processes. *Physical Review D*, 32(9):2380–2382, 1985.

[14] M. Diehl, D. Ostermeier, and A. Schäfer. Elements of a theory for multiparton interactions in QCD. *J. High Energ. Phys.*, 2012:89, 2012.

[15] A. V. Manohar and W. J. Waalewijn. QCD analysis of double parton scattering: spin and color correlations, interference effects, and evolution. *Phys. Rev. D*, 85:114009, 2012.

[16] M. Diehl, J. R. Gaunt, D. Ostermeier, P. Plößl, and A. Schäfer. Cancellation of Glauber gluon exchange in the double Drell-Yan process. *J. High Energ. Phys.*, 2016:76, 2016.

[17] M. Buffing, M. Diehl, and T. Kasemets. Transverse momentum in double parton scattering: factorisation, evolution and matching. arXiv:1708.03528, 2017.

[18] M. Diehl and T. Kasemets. Positivity bounds on double parton distributions. *J. High Energ. Phys.*, 2013:150, 2013.

[19] T. Kasemets and P. J. Mulders. Constraining double parton correlations and interferences. *Physical Review D*, 91(1), 2015.

[20] D. Binosi and L. Theussl. JaxoDraw: A graphical user interface for drawing Feynman diagrams. *Comput. Phys. Commun.*, 161:76, 2004.